Journal of Earthquake Science and Engineering

http://www.joes.org.in

Publisher ISES 2017 Journal of Earthquake Science and Engineering, vol. 4, pp 17 -34

SUBSIDENCE MAPPING RELATED TO COAL MINE FIRES IN THE JHARIA COAL FIELD (INDIA) USING ASTER TIR AND ERS SAR DATA

V. K. Srivastava[1], Salil Agarwal[1], and T. J. Majumdar[2*]

[1]*Department of Applied Geophysics, Indian School of Mines, Dhanbad – 826004, India*

[2]*Space Applications Centre (ISRO), Ahmedabad - 380015, India*

[*]Email: *tjmajumdar@rediffmail.com* (T. J. Majumdar, Ex-Scientist, SAC)

Abstract

Coal fires are common and serious phenomena in most coal-producing countries in the world. Coal fires not only burn valuable non-renewable coal reserves but also severely affect the local and global environment. The local impacts, some of them being irreversible, may concern environmental damage and degradation of land, heat effects on surrounding rocks and land subsidence, loss of forest cover, lowering of water quality, and the smoke-related air pollution which affect human health and safety. The famous Jharia Coal Field of Dhanbad, India is no exception where coal mine fire has been reported nearly a century back and still continuing unabated in vast area of the coal field. Therefore, the problem of coal mine fire needs to be studied and monitored using appropriate technique over the affected area in addition to the conventional techniques which is site specific, in general. Out of the various techniques, analysis of satellite remote sensing data collected in visible, near infrared, thermal infrared and microwave regions have been found to be very efficient and cost-effective in mapping and monitoring of the coal mine fires and associated environmental hazards; that too in comparatively less time.

An attempt has been made to analyse the high resolution multispectral thermal IR images of ASTER (Advanced Spaceborne Thermal Emission and reflection Radiometer) to prepare the surface temperature anomaly map and thus delineating surface and subsurface coal mine fire regions of the Jharia Coal Field. Further, the generated temperature gradient map as well as the surface temperature map have helped in differentiating shallow and deeper coal mine fire regions and surface heat features. The coal mine fire map reveals that the coal fire is distributed

mostly in the eastern part of the Jharia Coal Field, where two major coal fire zones have been delineated; one at Lodna–Tisra-Bhulanbarari-Kujama–Jealgora and the other one at Kusunda – Kendudih area. The western fire zone, on the other hand, is restricted in Dumra-Nadkhurkee-Jayramdih area. Based on the present study using ASTER thermal infrared data of 2006, the total active coal mine affected fire area in the Jharia Coal Field (India) has been estimated to be around 7 km^2 in which the deep subsurface coal mine fire area has been found to be around 3 km^2 whereas shallow surface coal mine fire area is found to be around 4 km^2 as compared to the coal mine fire area of 18 km^2 as estimated using Landsat TM thermal IR band data of 1987 with 120 m spatial resolution. This shows that the fire-affected region has been decreased by about fifty percent during the last 18 years. However, such decrease of coal fire has been observed in the central part only. On the other hand, an increase of coal fire has been observed in the south-eastern parts of the Jharia Coal Field.

Further study of Differential SAR Interferometry (DInSAR) map generated using ERS SAR tandem images over the Jharia Coal Field has helped in delineating the subsidence prone regions, which may be due to coal fire as well as due to some other reasons.

Keywords: Coal mine fire, Jharia coal field, Thermal remote sensing, ASTER, ERS SAR, DInSAR

1. Introduction

Coal fires, both underground and on the surface, are a serious problem in most major coal-producing countries of the world. A coal seam fire or mine fire is the underground slow burning of coal deposit, often in a coal seam/mine and propagate in a creeping fashion along mine shafts and cracks in geologic structures. The main cause of such coal mine fire is natural i.e. by way of spontaneous combustion and it could also occur sometimes due to human activities related with coal exploitation operations (Srivastava, 2004). Such fires have economic, social and ecological impacts.

Spontaneous combustion is a process of liberation of heat by the interaction of coal with oxygen of air in ambient temperature which, if allowed to accumulate would enhance the rate and ultimately lead to fire known as combustion of coal (Banerjee, 1985**;** Srivastava, 2004) and accumulation of such heat is favoured by poor conductivity of coal. It is also observed that spontaneous heating is facilitated where large mass of coal is involved and ventilation is neither too little to restrict coal oxygen interaction nor too big to dissipate away all the heat generated from the above (Banerjee, 1985). The risk of spontaneous combustion strongly depends on a number of external factors as well as on coal specific parameters which include e.g. coal rank (degree of coalification), petrographic composition, methane content, moisture content, as well as particle size and surface area. High coal rank, high content of original

oxidized plant material, a relatively large particle size and low specific internal surface decreases the coal's self-heating capacity (Ackersberg, 2003).

Geoenvironmental factors such as climate, geology and geomorphology also affect the self-heating process but need to be studied well. Once a coal fire starts in a coal seam it has a high potentiality to burn for a long time which spreads further along the strike and dip of the coal seam. Such coal fire, when start at the surface of an outcropping, dipping coal seam, causes overlying bedrocks to collapse, resulting in sufficient oxygen supply for the combustion of underground coal which may continue for decades.
Major coal fires of the world, largely uncontrolled, are burning in Asia and in India. Coal mining has started in the late 18th century in Raniganj (West Bengal), located near about 200 km northwest of Calcutta in what is now known as the Eastern coalfields. In the past 40 years or so the rate of coal extraction from Indian mines has been accelerated, putting India as the third largest coal producing country in the world.

Underground coal mine fires have been reported here for the past 100 years or more. Fires which are burning underground pose a much more serious situation to manage and have caused variety of environmental hazards /problems in the region. In addition, the volume loss caused by burned out coal seams often leads to land subsidence, landslides and the development of cracks or burned pits, posing a threat to local infrastructures and buildings. Subsidence is an inevitable phenomenon of ground movement caused by various manmade and natural activities. According to Zhang *et al.* (2004) land subsidence is mainly restricted to large coal fire areas, whilst significant subsidence rates are most probably caused by combined effects of both coal fires and coal mining. Further emission of gases due to burning of coal fires also contribute in decreasing the air quality.

Many researchers, such as Srivastava (2004), Srivastava *et al.* (2013), Bhattacharya and Reddy (1994), Cracknell and Mansoor (1992), Bhattacharya *et al.* (1991), Saraf *et al.* (1995) have mapped and delineated coal mine fires in the Jharia Coal Field (JCF) using multispectral and multitemporal remote sensing data. Bhattacharya *et al.* (1991) could distinguish the fires from the background using airborne predawn TIR and daytime multispectral data acquired by Daedalus Multi-Spectral Scanner. Mukherjee *et al.* (1991) attempted to estimate the depth of the fire from acquired predawn airborne thermal data using a liner heat flow equation. Cracknell and Mansoor (1992) used Landsat-5 TM and NOAA-9 AVHRR data and found that nighttime NOAA data was quite useful to isolate the warm areas from the background. Reddy and Bhattacharya (1995) used the short-wave infrared (SWIR) region of the electromagnetic spectrum, which recorded by Landsat TM bands 4, 5 and 7. They described that the hotspots found in the image corresponded well with the field measurements. In the same area, using Landsat TM bands 6 and 7, Saraf *et al.* (1995) found that comparatively high temperature zones must have surface fires, whereas the less warm areas should have subsurface fires. Later,

Prakash *et al.* (1995, 1997) and Prakash and Gupta (1999) used the Landsat TM TIR and SWIR bands to identify surface and subsurface fires separately, and attempted a method for calculating the area of surface fires. However the main problem they faced while developing this method was reflected solar energy in the SWIR region in the daytime images. Using concept of Coal Fire Radiative Energy (CFRE) in remote sensing, Tetzlaff (2004) and Voigt *et al.* (2004) have studied the characteristics and importance of ASTER, BIRD and ETM data in modelling coal mine fire spots in Chinese coal field region. Nighttime thermal IR data of an area removes the effect of differential heating of terrain surface which helps in delineating associated surface thermal features relating to underground coal mine fires with less ambiguity. Chatterjee et al. (2015) have used spaceborne differential interferometric SAR, GPS and precision levelling techniques for detecting, mapping and monitoring of land subsidence in Jharia Coalfield, Jharkhand, India.

Considering such serious environmental impacts and other valuable loss of precious prime coking coal, it is necessary to map and monitor the status of coal mine fires in the JCF, India using suitable advanced techniques for better scientific planning, management and combating of fires providing sustainable environment development in the region.

2. Study area, regional geology, coal mine fires and environmental hazards

The JCF, which is the only important prime coking coal source of India, is situated in the district of Dhanbad (Jharkhand) about 260 km NW of Kolkata on the northern margin of Damodar Valley. This coal field is roughly sickle shaped and extends for about 38 km in an east-west direction and approximately 18 km in north-south direction covering an area of about 456 km^2. Coal mine fires in this coal field has been reported nearly a century back. Fire occurrence was first reported in 1916. In the JCF, about 1864 million tonnes of coal is lying blocked in about 65 fire spots spread over area of 17.32 km^2. This includes not only the area under fire but also the area which has been sealed off due to heating and since then has not been opened (Singh, 2013). Accordingly, the whole area has become subsidence prone.

Regional geology of the area constitutes lower Gondwana sedimentary rocks surrounded by Archaean metamorphic and granitic rocks with presence of intermittent boulder of dykes over eroded peneplain low sloping terrain (Fig. 1). The general stratigraphic succession of the area is that the basement metamorphic rocks are overlain by the Talchir formation followed by the Barakar Formation which is the main coal bearing horizon. Above it, comes the Barren Measures which is followed by the coal-bearing Raniganj Formation. The coal of the Raniganj Formation have slightly higher moisture content than the coal of the Barakar Formation.

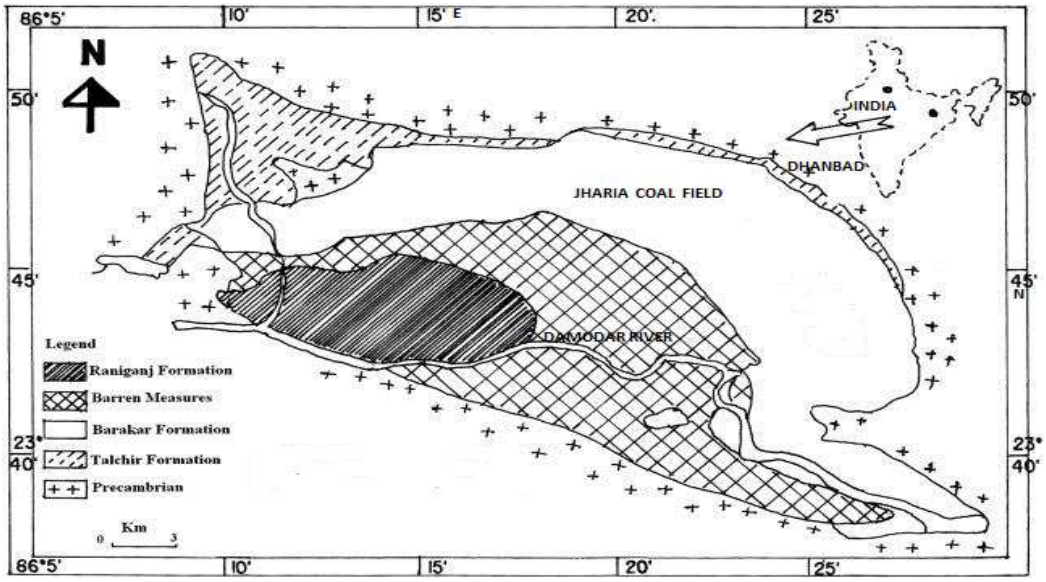

Fig. 1: Geological map of the Jharia Coal Field

In Jharia, the upper coal seam has less ash contain than the lower one and these have been mined extensively. Unfortunately these upper seams are very susceptible to spontaneous combustion, resulting in coal mine fires (Srivastava, 2004). These fires (Fig. 2) in Jharia often extend upwards to the land surface.

Finally once the fire breaks out, it reaches to surface and then it becomes difficult to control particularly due to the synergetic effect of underground combustion, strata fracture and subsidence with flow of air from the surface through subsidence cracks.

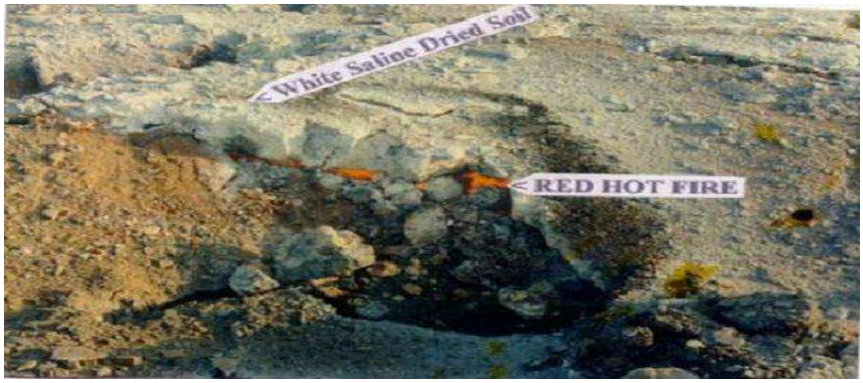

Fig. 2: Typical surface coal mine fire seen as orange red tone and surface soil (dried) with salt deposit as shown by white tone.

Unplanned and haphazard mining operations as well as mine based industry in the area have triggered environmental hazards like surface subsidence, loss of vegetation cover and

associated soil erosion in mining site, changes in landscape due to dumping of coal and waste materials, water pollution, changes in surface and subsurface hydrologic system, noise pollution and coal mining fires in both underground and in surface coal dumps. It also endanger the surface civil structures, damage to surface vegetation, health hazards due to emission of poisonous gases and when fire burns for longer period, it degrades the air quality by releasing pollutants such as carbon monoxide (CO), carbon-dioxide (CO_2), methane (CH_4), sulphur-dioxide (SO_2) as well as toxic gases like hydrogen sulphide (H_2S) and nitrous oxide (N_2O) and particulate materials. The gaseous emissions are a long-term health threat for the local population and contribute to the problem of global warming. By knowing the exact status of coal mine fire area in the JCF, better planning and management programs can be made to control coal mine fire.

3. Materials and Methods

The facts that the coal mine fires causes ground heating and thus generates detectable surface thermal anomaly compared to the background could be easily detected by thermal infrared sensors on-board airplane or satellite. However some of these coal fires on the surface, when present as flaming combustion, emit significant thermal energy that is easy to detect by any remote sensing scanner. Out of these, some may be at high enough temperature to become visible in wavelength bands shorter than the thermal infrared.

We have used here radiometrically calibrated and geometrically corrected - Level 1B data of night pass ASTER multi-band Thermal IR (TIR) data of Dec. 2006 on-board the multi-sensor Japanese TERRA satellite maintained by Earth Resources Satellite Data Agency (ERSDAC), Japan. The data has five thermal infrared channels viz.; with spatial resolution of 90 m which is higher compared to Landsat TM TIR data (~120 m). Accordingly, the results obtained here in the JCF are expected to be better than the earlier one. Details of ASTER bands is given in Table 1.

Table 1: Different bands of ASTER and their specifications

Band	Wavelength (μm)	
Visible and near infrared		8 bit integer
Band 1	0.52–0.60	
Band 2	0.63–0.69	Spatial resolution 15m
Band 3N (3B)	0.76–0.86	Swath width 60 km

VNIR band has 2 bands (3N and 3B), which are stereo pair images.

Short wave infrared

8 bit integer

Band 4 1.600–1.700
Band 5 2.145–2.185 Spatial resolution 30m
Band 6 2.185–2.225 Swath width 60 km
Band 7 2.235–2.285
Band 8 2.295–2.365
Band 9 2.360–2.430

Thermal infrared

12 bit integer

Band 10 8.125–8.475
Band 11 8.475–8.825 Spatial resolution 90m
Band 12 8.925–9.275 Swath width 60 km
Band 13 10.25–10.95
Band 14 10.95–11.65

3.1 Methodology for coal fire mapping/monitoring using ASTER TIR/Landsat data

Thermal infrared (TIR) radiation of an object is controlled mainly by several factors viz. the emissivity of the object, its geometry and its temperature. A perfect blackbody has a predictable range of wavelengths that vary with the temperature in degree Kelvin, and that moves to shorter wavelengths as the temperature increases. For objects with an emissivity of 1, the observed "brightness temperature" is equivalent to the kinetic temperature of the object. So the conversion from brightness (remotely observed) temperature to kinetic temperature can be made when the characteristic emissivity of an object is known. The methods and techniques of converting DN values into the Brightness Temperatures and further to Radiative Fire Energy (FRE) have been discussed in detail by Tetzlaff (2004). Standard basic equations have been used here for converting DN values into the corresponding Brightness Temperatures.

All materials above absolute zero temperature emit radiation. A perfect emitter, the so-called "blackbody", emits the maximum amount of radiation at each wavelength. In nature, no material is perfect emitter or absorber and so the emissivity (e) of natural material describes how closely its emittance relates to a standard blackbody:

$$\varepsilon_{\lambda,T} = \frac{L_{gb,\lambda}(T)}{L_{bb,\lambda}(T)} \quad \ldots \quad \ldots \quad \ldots (1)$$

where:

Ελ,T = emissivity at a certain wavelength and temperature.

Lgb,λ(T) = real radiance at a certain wavelength and temperature

Lbb,λ(T) = blackbody radiance at a certain wavelength and temperature

The emissivity is a function of both temperature and wavelength. The spectral radiance emitted by a blackbody, at a temperature (T), is given by the Planck Function as:

$$L_{bb} = \frac{c_1}{\lambda^5 \pi [e^{c_2/\lambda T} - 1]} \quad \ldots \quad \ldots \quad \ldots (2)$$

where:

Lbb = blackbody radiance [W m-2 sr-1 μm-1]

λ = wavelength [m]

T = temperature [K]

c1 = first radiation constant: 3.742 x 10-22 [W m3 μm-1]

c2 = second radiation constant: 0.014 [m K]

For each temperature the Planck Function has maximum emission at certain wavelength:

$$\lambda_m = \frac{2897.9}{T} \quad \ldots \quad \ldots \quad \ldots (3)$$

where:

λm = wavelength of maximum emission for a blackbody [μm]

First, the DN values have to be converted to sensor radiance and then sensor radiance can be converted to brightness temperature using the following equation:

$$T = \frac{K_2}{\ln\left(\frac{K_1}{L_\lambda} + 1\right)} \quad \ldots \quad \ldots \quad \ldots (4)$$

K_1 and K_2 are the coefficients determined by effective wavelength of a satellite sensor.
For example, effective wavelength of ASTER band 10, l=8.291 μm = 8.291×10-6 m, we can have K_1 = C1/λ5 = 1.19104356×10-16 W m2/ (8.291×10-6 m)^5 = 3040136402 W m-2 m-1 = 3040.136 W m-2 μm-1 $K_2 = C_2/\lambda$ =1.43876869×10-2 mK /8.291×10-6 m = 1735.33K.

3.2 Methodology for DEM generation using ERS SAR tandem data for subsidence mapping/monitoring

Radar interferometry offers a unique means of mapping ground movements. The technique uses the phase of radar images as a measure of distances from ground to the satellite bearing instrument. Accuracies of the order of radar wavelength (~ cm) are obtained with these measurements. The important parameters include contributions from (i) trajectories, (ii) topography, (iii) ground movements, (iv) atmosphere, and (v) others, including instrumental contributions. Srivastava (1997) had already mapped the detailed drainage patterns over the JCF using remote sensing methods which has a direct linkage to the neotectonic features in this region.

Monitoring dynamic topographic changes in a hazard-prone mining belt is a critical activity for land environmental management. Such temporal topographic changes over a period of time and even for short-term mining activity, say, within a year, could be carried out using a Digital Elevation Model (DEM) generated using various space-borne techniques (Srivastava *et al.* 2012). Among all techniques available for generating DEM, the SAR Interferometry technique has been particularly successful and effective, offering high resolution spatial detail to a level of a few cm.

SAR interferometry or InSAR is a technique for extracting topographic information from complex radar signals. It exploits the phase differences of two complex-valued SAR images acquired from different orbit positions and/or at different times. Topographic information about the scene is obtained by differencing the phase of each pixel. Due to vertical separation between the receiving antennas, phase differences can be observed which can later be converted to pixel height. Pixel height (h), and phase difference (Φ) are related by the following equations (Zebkar and Goldstein, 1986; Srivastava *et al.* 2012):

$$\Phi = 4\pi/\lambda \, [Bx \sin \theta - By \cos \theta] \quad \ldots \quad \ldots \quad \ldots (5)$$

$$h = H - r \cos \theta \quad \ldots \quad \ldots \quad \ldots (6)$$

where λ is the radar wavelength and B is the baseline.

The phase difference of the two SAR images (ERS-SAR (European Remote sensing Satellite - Synthetic Aperture Radar) working in C band, in the present case) is calculated for an interferogram where fringes represent the whole range of the phase from 0 to 2π in a full colour cycle. The correlation of the phase information of two SAR images is measured as coherence in the range of 0 to 1. The degree of coherence can be used as a quality measure because it significantly influences the accuracy of phase difference and height measurements. The phase information is directly related to the topography. Several workers have successfully used the InSAR technique (Majumdar and Massonnet, 2002; Gupta *et al.* 2007; Srivastava *et al.* 2012) for DEM generation/monitoring.

Initially, InSAR technique was implemented using ERS tandem data set of April 12 and April 13, 1995 and then further using ERS tandem data set of May 16 and 17, 1996 passes.

4. Results

After converting DN values into brightness temperature, it is observed that the maximum pixels represent a brightness temperature of 289 K or 16°C which has been taken as background brightness temperature in the area (as shown by square box in Fig. 3). This figure shows colour coded thermal infrared brightness temperature anomaly map of the JCF where the red tone represents the high thermal anomaly areas and the blue tone represents background thermal anomalous region.

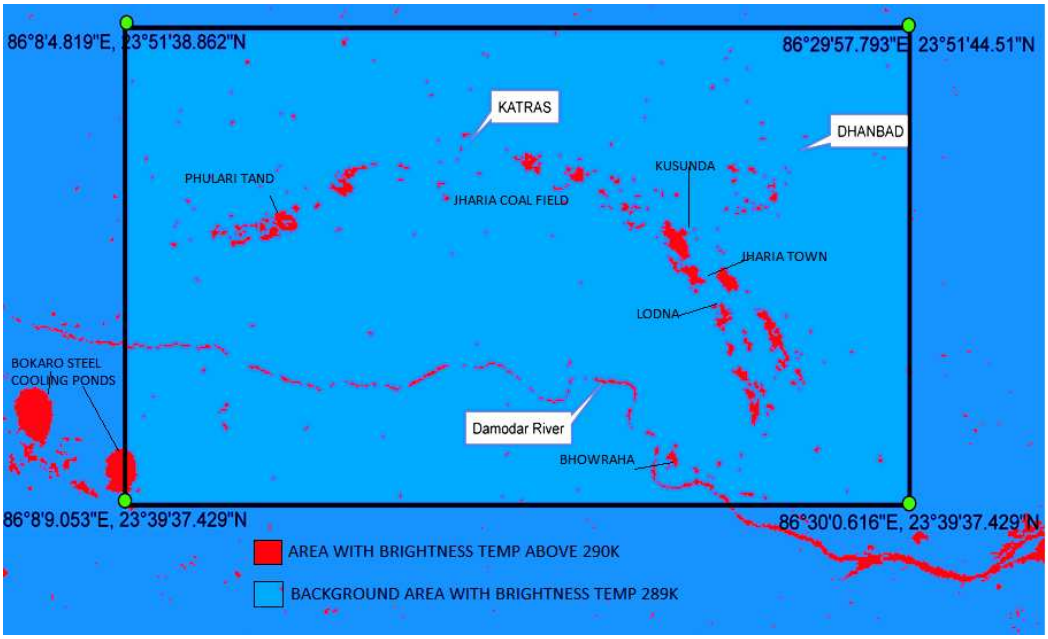

Fig. 3. Pixels having Brightness Temperature above 290K have been classified in red tone and pixels representing all features equal to or below 289K are shown in blue tone

The high thermal anomaly map (shown by red tone in Fig. 3) has been further classified into two zones viz.; shallow features representing brightness temp in range 291-292 K and above 293 K as deep seated features showing brightness temp below 292 K as shown in Fig. 4.

In this figure, the blue tone represents features with brightness temperature equivalent to 291 - 292K or less within high anomaly map and after checking it is observed that these features are mainly cultural features or surface water bodies like rivers etc. This is because the water body absorbs most of the solar radiation falling on it therefore its temperature generally increases compared to the surrounding background temperature (in this case background surface brightness temperature is 289K) or the features could be due to deep subsurface coal mine fires.

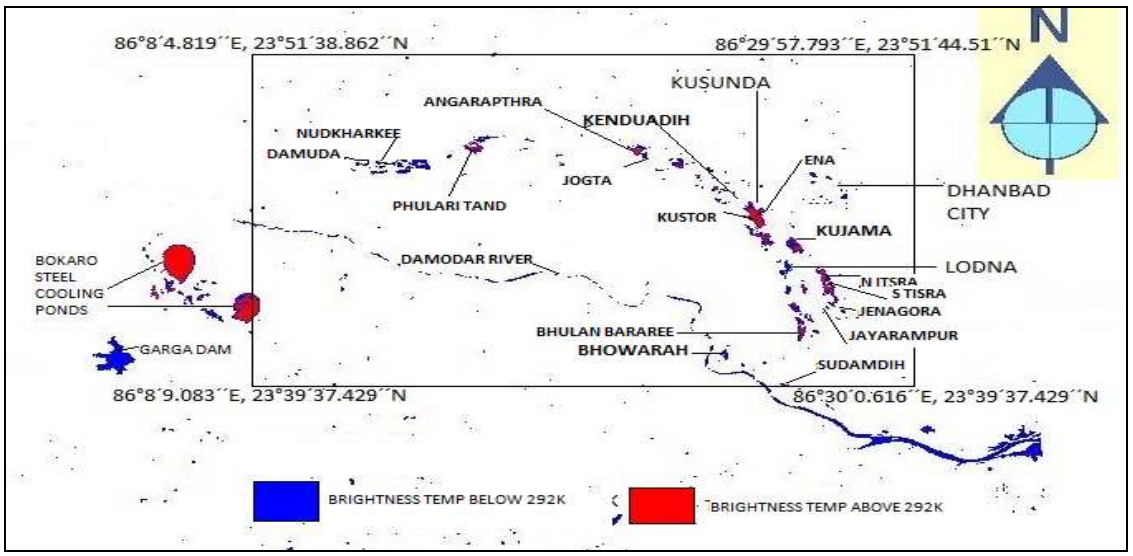

Fig. 4: This fire map shows two classes of high temperature anomaly within the high heat areas as delineated in Fig. 3.

Further, another class of high temperature anomaly map with brightness temperature above 292 K has been delineated in Fig. 4 as red tone. After checking, it is observed that such anomaly either represents deep fire inflame spots or high heated cultural features such as steel plant ponds, brick kline, coal washeries, etc. Thus the confusion in classifying pixels/region due to deep coal mine fires and surface fires cultural activities have been solved to certain extent after generating temperature gradient map as shown in Fig. 5 and discussed below.

4.1 Analysis of Temperature Gradient Map to identify/differentiate shallow and deep fire zones

Considering the general principle that a shallow surface coal fire will have a steep gradient with high peak; a deep subsurface fire will have a lesser gradient anomaly of low peak where as the man-made structures and water bodies will have a steep gradient at the boundary but will have near zero gradient within the spatial extent of surface features, the temperature (surface) gradient map has been generated and discussed here. So this map (Fig. 5) has been studied for separating out various features viz.; heated bodies of shallow, deep and cultural features within the high heat anomalous zones. From Fig. 5, it is clear that man-made structure like steel plant cooling ponds and water bodies, Ganga Dam and Damodar River have steep gradient at the boundary but has a near zero temperature gradient inside the features i.e.these bodies are of constant/uniform temperature i.e. of flat gradient bodies, whereas area showing discontinuous high gradient anomalous features with very close spacing temperature contours show shallow surface coal fire areas. But the deep in seam coal fires are shown by low peaked wide spacing temperature gradient surface anomaly contours within the JCF. Therefore, such temperature gradient map has been found useful in differentiating shallow and deep coal mine fire areas from other high temperature bodies like cultural features and uniform water bodies.

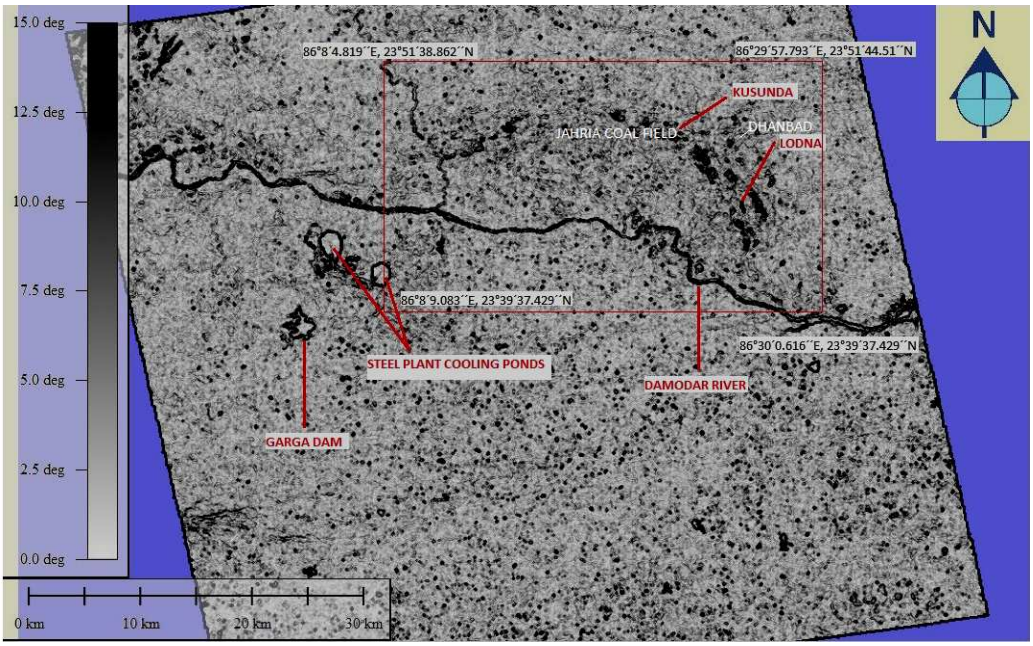

Fig. 5: Brightness Temperature Gradient Map

4.2 Comparative status of aerial extent of Coal Mine Fire in Jharia since 1987 as delineated using Landsat TM TIR band

On the basis of daytime Landsat TM thermal band data of 1987 with spatial resolution of 120 m, Srivastava (1996) estimated that the areal extent of active coal mine fire in the JCF was around 18 km^2 (Fig. 6) which is shown here with blue colour tone in the Figure on which

coal mine fire areas as delineated from the present study of ASTER TIR data of 2006 (night pass) has been overlaid as shown by hatched brown colour. After comparison it is observed that the fire areas in western and central part of the coal field have been reduced since 1996 whereas in eastern part, no improvement in the status has been observed.

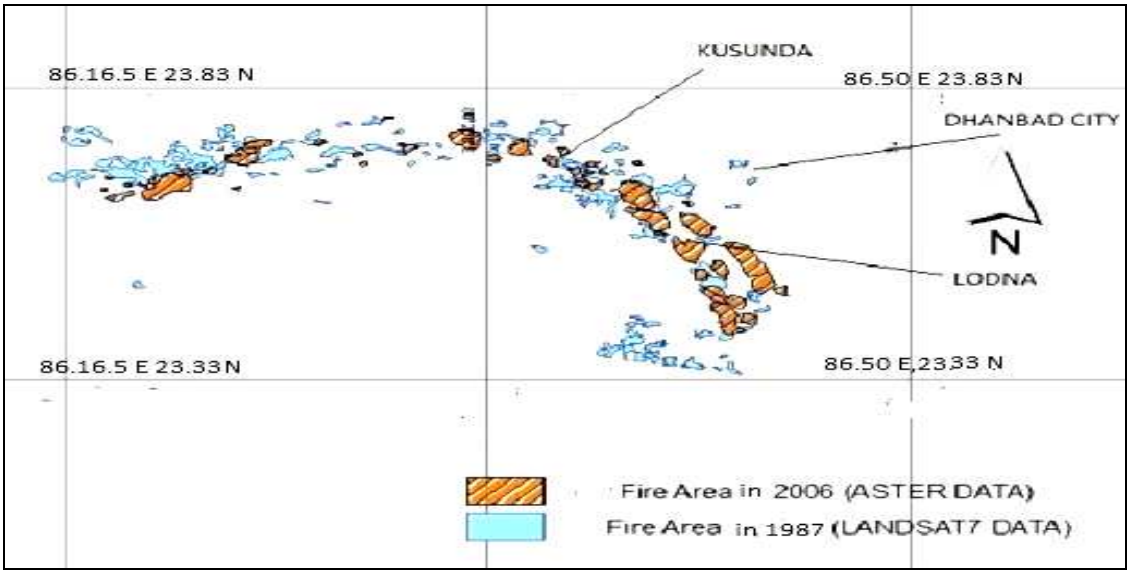

Fig. 6. Status of coal mine fire area in the Jharia Coal Field as delineated (in blue tone) using Landsat TM TIR data of 1987 and status of 2006 as shown by hatched brown colour tone using ASTER TIR data

It is estimated that the areal extent of active coal mine fire in the JCF is around 7 km^2 in 2006 using ASTER band of 90 m resolution data out of which the deep subsurface coal mine fire area in Jharia coalfield is around 3 km^2; whereas shallow surface coal mine fire area is found to be around 4 km^2. The study has shown that the there has been reduction in fire affected areas by 60 to 65 percent in the study area since last 20-25 years.

4.3 Study of DEM as generated from InSAR Tandem data sets

Initially DEM of the area was generated with InSAR technique using tandem data set of April 12 and April 13, 1995 and then further using ERS tandem data set of May 16 and 17, 1996 passes, another set of inteferogram of the area was generated in order to get DInSAR map over the JCF, integrating information from ground control points and precise high coherence orbital parameters as discussed by Srivastava *et al.* (2012). InSAR image generated over the study area of interest is shown in Fig. 7. Figure 8 shows the merged product of IRS LISS III

and PAN draped over DEM as generated using InSAR technique after Gupta *et al.* (2007), and Srivastava *et al.* (2012). Significantly, the intense coal mine fire areas are correlating well with mine subsidence (Fig. 8). In the merged product, fringes represent the whole range of the phase from 0 to 2π in a full colour cycle. This indicates that the active fire area is associated with low topography in the region.

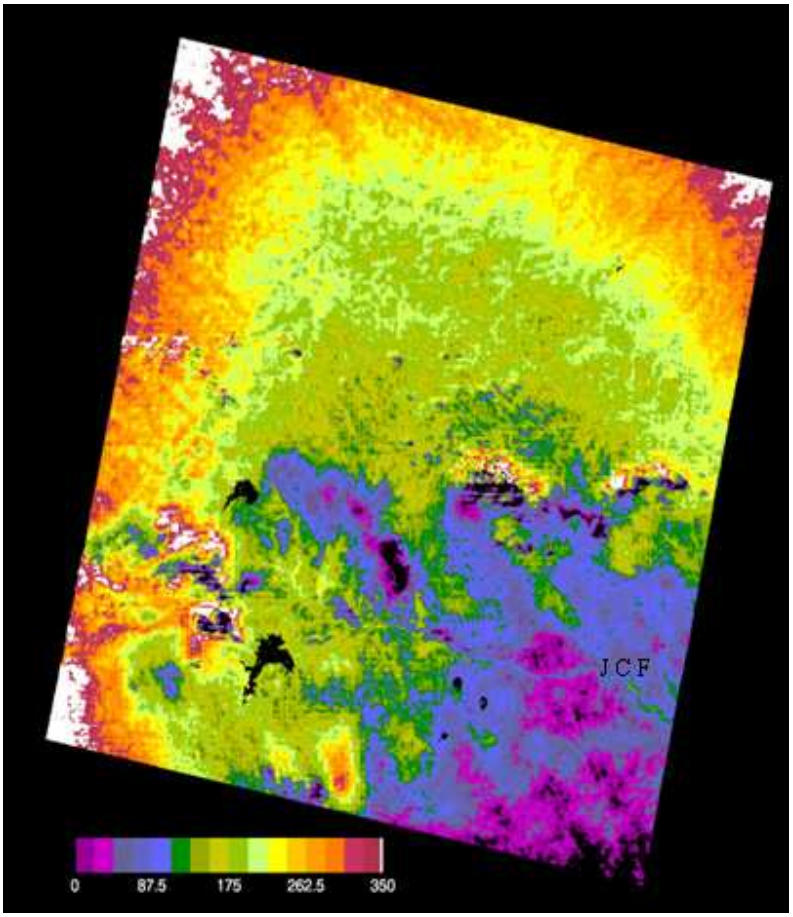

Fig. 7. InSAR image as generated over the Jharia Coalfield (JCF)

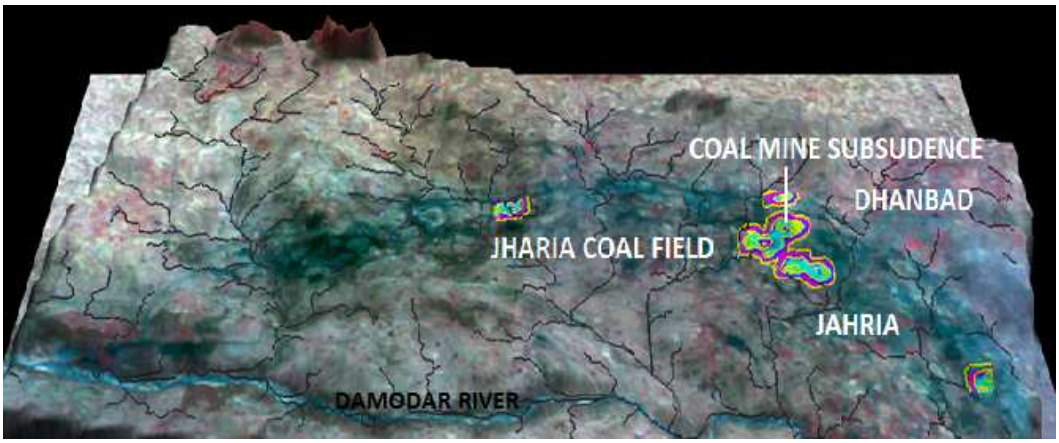

Fig. 8. Merged product of IRS LISS III and PAN draped over DEM as generated using InSAR technique after Gupta *et al.* (2007) and Srivastava *et al.* (2012).

5. Discussion and Concluding Remarks

From the study of various thematic thermal maps as generated using ASTER image data of 2006 and of Landsat TM thermal IR data of 1987 following results have been obtained.

The coal mine fire region as delineated from ASTER images has been classified into three categories: (1) high intensity zone representing shallow surface fires or may be inflame fires on surface associated with brightness temperature >292K, (2) medium intensity zone indicating subsurface fires associated with brightness temperature = 291 and 292K and (3) low intensity zone representing background region associated with brightness temperature (=289 K or less) during the nighttime. The generated temperature gradient map has provided further criteria viz.; a) steep gradient with high peak i.e. closed spaced gradient contours, b) low gradient with low intensity peak i.e. wide spaced gradient contours and c) low flat gradient at the rim with wide spaced surface temperature gradient contours within the features which show surface shallow coal mine fires area to the deeper coal mine fire areas as well as from other high heated erroneous cultural features respectively. The coal mine fire map reveals that the coal fire is distributed mostly in the eastern part of the JCF. Two major coal fire zones are present in the eastern part of the JCF, one is Lodna–Tisra-Bhulanbarari-Kujama–Jenagora and other is Kusunda – Kendudih area. The western fire zone on the other hand is restricted in Dumra-Nadkhurkee-Jayramdih area. The coal mine fire area has decreased in western and central part of the JCF but it has increased considerable in some eastern parts (see Figs. 3 and 4).

It is estimated that the areal extent of active coal mine fire in the JCF is around 7 km^2 in 2006 out of which the deep subsurface coal mine fire area in the JCF is around 3 km^2.and the shallow surface coal mine fire area is around 4 km^2, compared to 18 km^2 coal mine fire areas in total in 1987 obtained using Landsat TM TIR data. From the study, it is concluded that the

analysis of ASTER multi-band thermal imagery have been of much help in delineating high heat areas as well as knowing the type and nature of coal mine fires in the study area of the JCF.

InSAR DEM study has shown that some of these delineated fire regions in the eastern part of the coalfield near Kusunda is associated with low topography. Study of high resolution DInSAR images have been of further help in monitoring and measuring land topography in the region due to subsidence which appear to be associated with active mine fires. In the merged product, fringes represent the whole range of the phase from 0 to 2π in a full colour cycle which again indicates the association of the active fire areas with low topography. Usage of latest data e.g. Sentinel SAR/TIR (Sentinel 1/3) data may enhance the technique further.

Acknowledgements

Authors (SA and VKS) wish to thank the Director, Indian School of Mines, Dhanbad,India for providing all facilities. TJM wishes to thank CSIR, New Delhi for Emeritus Scientist Fellowship since January 2011. Authors are also thankful to Dr. A. K. Saraf, IIT, Roorkee for his critical comments which has helped in improving the manuscript. This paper is an update of *Mapping of coal mine fires and resulting subsidence in the Jharia coal field (India) using ASTER multispectral thermal IR data and ERS SAR images*, published in the World Mining Congress 2013 Proceedings. Updated and submitted with permission from the Canadian Institute of Mining, Metallurgy and Petroleum.

References

Ackersberg, R. (2003) Understanding self-ignition of coal. Internal unpublished project report, German Montan Technology and Federal Institute for Materials Research and Testing, Germany.

Banerjee, S. C. (Ed.) (1985) Spontaneous combustion of coal and mine fires, *Oxford & IBH Publishing Co. India*, 168 p.

Bhattacharya, A., C. S. Reddy and T. K. Mukherjee (1991) Multi-tier remote sensing data analysis for coal mine fire mapping in Jharia coalfield of Bihar, India, *Proc. 12th Asian Conference on Remote Sensing,* Singapore, Oct.' 91, pp. 221-226.

Bhattacharya, A. and C. S. Reddy (1994) Underground and surface coal mine fires in India's Jharia coal field using thermal infrared data, *Asian Pacific Rem. Sens. J.,* 7(1), 59-73.

Chatterjee, R. S., S. Thapa, K, B. Singh, G. Varunakumar and E. V. R. Raju (2015) Detecting, mapping and monitoring of land subsidence in Jharia Coalfield, Jharkhand, India by spaceborne differential interferometric SAR, GPS and precision levelling techniques. *J. Earth Syst. Sci.* 124, No. 6, 1359–1376.

Cracknell, A. P. and S. B. Mansoor (1992) Detection of subsurface coal fires using Landsat Thematic Mapper data, *Int. Archive Photogramm & Rem. Sens.,* 29(B7), 750-753.

Gupta , M., K. K. Mohanty and T. J. Majumdar (2007) Land subsidence mapping in Jharia coalfield using InSAR and DGPS measurements, Conference of Joint Experiment Project towards Microwave Remote Sensing Data Utilization (JEP-MW). May 15-16, 2007, SAC, Ahmedabad, SAC Report no. SAC/RSMET/JEPMW/CP/03/2007, pp. 7-21 to 7-30.

Majumdar, T. J. and D. Massonnet (2002) D-InSAR applications for monitoring of geological hazards with special reference to Latur earthquake, 1993, *Curr. Sci.,* 83 (4), 502-508.

Mukherjee, T. K., T. K. Bandyopadhyay and S. K. Pandey (1991) Detection and delineation of depth of subsurface coal mine fires based on an air-borne multispectral scanner survey in a part of Jharia coal field, India, *Photogramm. Engg. & Rem. Sens.,* 57(9), 1203-1207.

Prakash, A., A. K. Saraf, R. P. Gupta, M. Dutta and R. M. Sundram (1995) Surface thermal anomalies with underground fires in Jharia coal mine, India, *Int. J. Rem. Sens*., 16, 2105-2109.

Prakash, A., R. P. Gupta, and A. K. Saraf (1997) A Landsat TM based comparative study of surface and subsurface fires in the Jharia coalfield, India, *Int. J. Rem. Sens*., 18, 2463-2469.

Prakash, A. and R. P. Gupta (1999) Surface fires in the Jharia coalfield, India-their distribution and estimation of area and temperature from TM data, *Int. J. Rem. Sens.,* 20, 1935-1946.

Reddy, C. S. and A. Bhattacharya (1995) Use of GPS for ground truth data collection and its integration with RS and GIS :A case study with reference to mine fires in Jharia, Bihar State, India, *Asia Pacific Rem. Sens. J.,* 7, 155-158.

Saraf, A. K., A. Prakash, S. Sengupta and R. P. Gupta (1995) Landsat-TM data for estimating ground temperature and depth of sub-surface coal fire in the Jharia coal field, India, *Int. J. Rem. Sens*., 16, 2111-2124.

Singh, R. V. K. (2013) Spontaneous heating and fire in coal mines. *Procedia Engg.,* 62, 78 – 90.

Srivastava, V. K. (1996) Application of Landsat-TM thermal band and IRS-1A LISS II imagery in delineation of coal mine fire in Jharia Coal Field, *Geospatial World Proceedings,* AASC.

Srivastava, V. K. (1997) Study of drainage pattern of Jharia coalfield (Bihar), India, through remote sensing technology, *J. Ind. Soc. Rem. Sens.,* 25 (1), 41- 46.

Srivastava, V. K. (2004) Natural disaster management through thermal remote sensing, GIS and GPS in reference to coal mine fire hazards, *Proc. World Congress on Natural Disaster Mitigation*, Feb. 2004, New Delhi , V. 1, pp. 258-262.

Srivastava, V. K., K. M. Sreejith and T. J. Majumdar (2012) Utilisation of ERS SAR data over the Jharia Coalfield (Dhanbad), India for subsidence monitoring, *Space Res. Today*, 85, 98-104.

Srivastava, V. K., S. Agarwal and T. J. Majumdar (2013) Mapping of coal mine fires and resulting subsidence in the Jharia coal field (India) using ASTER multispectral thermal IR and ERS SAR images, *Proc. 23rd World Mining Congress*, Montreal, Canada, Aug. 11-15, 2013, 11 p.

Tetzlaff, A. (2004) Coal fire quantification using ASTER, ETM and BIRD satellite instrument data, Ph. D. Dissertation submitted to Faculty of Science, LMU, Münichen, 179 p.

Voigt, S., A. Tetzlaff, J. Zhang, C. Kuenzer, B. Zhukov, G. Strunz, D. Oertel, A. Roth, P. Van Dijk and H. Mehl (2004) Integrating satellite remote sensing techniques for detection and analysis of uncontrolled coal seam fires in North China, *Int. J. Coal Geol.,* 59, 121-136.

Zebkar, H.A., and Goldstein, R. M. (1986) Topographic mapping from interferometric synthetic aperture radar observations. *J. Geophys. Res.,* 91 (B5), 4993-4999.

Zhang, J., W. Wagner, A. Prakash, H. Mehl and S. Voigt (2004) Detecting coal fire using remote sensing techniques, *Int. J. Rem. Sens.,* 25, 3193-3220.